doi:10.1246/cl.2012.860

Published on the web August 11, 2012

DFT Analysis of Low-frequency Heme Vibrations in Soluble Guanylate Cyclase: Raman Mode Enhancement by Propionate–Protein Interactions

Minoru Kubo,*[1] Orio Okuyama,[1] Teizo Kitagawa,[1] and Yasuteru Shigeta*[1,2]
[1]*Picobiology Institute, Graduate School of Life Science, University of Hyogo, Hyogo 678-1297*
[2]*Graduate School of Engineering Science, Osaka University, Toyonaka, Osaka 560-8531*

(Received April 16, 2012; CL-120335; E-mail: shigeta@cheng.es.osaka-u.ac.jp, mkubo@sci.u-hyogo.ac.jp)

Normal vibrational modes of heme have been analyzed using density functional theory, to assign a new Raman band observed at 312 cm^{-1} in the CO-bound, active form of soluble guanylate cyclase. The conserved YxSxR motif is incorporated into the model to reproduce the hydrogen-bonding network around propionates. A delocalized mode that involves Arg motions as well as pyrrole tilting and propionate bending is found to be the most likely candidate accounting for the new band.

Soluble guanylate cyclase (sGC) is the only known nitric oxide (NO) sensor protein and catalyzes the conversion of guanosine triphosphate (GTP) to cyclic guanosine monophosphate (cGMP), a second messenger regulating many cellular processes.[1] This enzyme is composed of α and β subunits and contains a heme, ligated by His105 in the β subunit, to sense NO.[2] NO binding to the heme ruptures the Fe–His bond due to the strong trans effect of NO,[3] which has long been inferred to trigger the enzyme activation.

Carbon monoxide (CO), being identified as a neurotransmitter, also binds to the heme and activates sGC when 3-(5′-hydroxymethyl-2′-furyl)-1-benzylindazole (YC-1), an allosteric activator, is present.[4] However, in the case of synergistic activation by CO and YC-1, the Fe–His bond remains intact in the major species.[5] This raises questions of how sGC can be activated without the Fe–His bond cleavage and what is a (real) factor triggering the activation.

To address these questions, resonance Raman (rR) spectroscopy is a powerful technique, because resonance enhancement provides high sensitivity and specificity for probing structural changes in heme and its vicinity. Although the binding site of YC-1 remains to be identified, deletion mutagenesis demonstrated that the α subunit is involved in YC-1 binding.[6] Thus, YC-1 perturbs the structure of heme active site allosterically. An rR spectrum of His-ligated, six-coordinate (6c) sGC–CO in the presence of YC-1 has been reported and characterized by strong resonance enhancement of a band at 312 cm^{-1} with Soret excitation.[5] Importantly, this band is resonance enhanced only in the presence of YC-1, namely, only in the active form. Therefore, assignment of this band will shed light on a key structural change in the heme active site for the enzyme activation. However, this band has not been assigned yet.

In this letter, we analyze low-frequency normal modes of heme at the density functional theory (DFT) level to understand the origin of the 312 cm^{-1} Raman band. Since this band is not normally observed for 6c heme systems, the resonance enhancement of this band should arise from the protein environment unique to sGC and may be related to the signal transduction pathway.

sGC belongs to a recently discovered class of H-NOX (heme-nitric oxide/oxygen binding) proteins, which share the conserved Tyr–Ser–Arg (YxSxR) motif that forms a hydrogen-bonding network with heme propionates.[7] Although a crystal structure of sGC is not yet available despite considerable efforts, that of Tar4, an H-NOX family member from *Thermoanaerobacter tengcongensis*, has been solved in the O_2-bound state.[7] The low-frequency rR spectrum of 6c Tar4–CO[8] resembles that of 6c sGC–CO with YC-1,[5] except that the 312 cm^{-1} band is relatively weak and that two vinyl-bending bands at 398 and 433 cm^{-1} are almost merged at ca. 420 cm^{-1} for Tar4. Accordingly, we constructed a 6c H-NOX heme model that has a ferrous heme with CO and imidazole (Im) as axial ligands and includes a triad of the YxSxR motif (Tyr131, Ser133, and Arg135) from the crystal structure of Tar4 (PDBID 1U55). Iron(II)–octamethylporphyrin with Im and CO ligation, CO·Fe(OMP)·Im, was also built as a reference system to analyze porphyrin vibrations.

Geometry optimizations and normal mode analyses were performed with Gaussian 09[9] using the B3LYP functional and 6-31G* basis set for all the atoms except Fe and the axial CO, for which Ahlrichs' VTZ basis set[10] was employed based on previous studies.[11] The structure of H-NOX heme model was optimized on the condition that the C_α and C_β atoms of the amino acids were fixed. On the other hand, the structure of the reference CO·Fe(OMP)·Im was optimized under the C_s symmetry, where the Im ring was put on the mirror plane. The spin state of the heme fragment is low spin, and $S = 0$ for both the models. Normal mode calculations yielded no imaginary frequencies, and all of the frequency values were taken directly from the Gaussian program without scaling.

Figure 1A shows the optimized structure of the H-NOX heme model, where the heme plane is somewhat relaxed from the distorted initial structure. Note that 6c Tar4–O_2 displayed strong out-of-plane (oop) heme bands near 700 cm^{-1} in the rR spectrum,[8] whereas 6c sGC–CO with YC-1 and 6c Tar4–CO did not,[5,8] which implies no significant heme distortion in the CO-bound state. Thus, care was not taken to hold the heme distortion during the optimization. However, a small (0.1 Å), but potentially important, oop tilt of the pyrrole D remains (Figure 1B) due to two hydrogen bonds between the 7-propionate and Arg. Consequently, this structure serves as a simple model to investigate heme vibrations perturbed by the YxSxR motif.

The H-NOX heme model has 81 vibrational modes below 400 cm^{-1}. The mode frequencies and polarizability derivatives (i.e., Raman activity) in a frequency range of 200 to 400 cm^{-1} are shown in Figure 2A. Raman-active modes are of current interest, but the calculated Raman activity corresponds to the nonresonance Raman intensity. In principle, in-plane (ip) porphyrin modes are enhanced in rR spectra of 6c hemes with

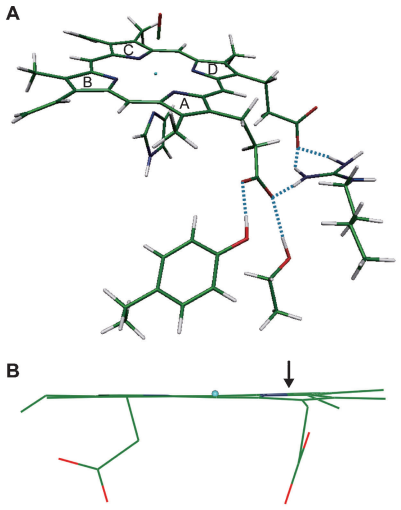

Figure 1. (A) H-NOX heme model. Cyan broken lines show hydrogen bonds. (B) Pyrrole D tilt of heme.

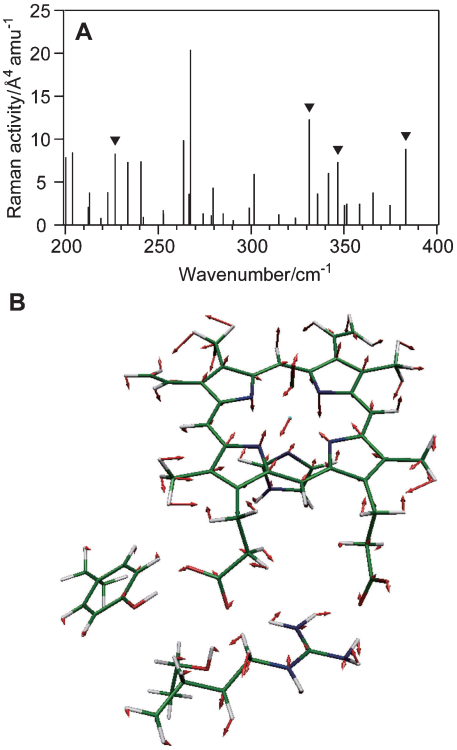

Figure 2. (A) Raman activity of the H-NOX heme modes in the 200–400 cm^{-1} region. Four Raman-active modes are marked with arrow heads. See the text for details. (B) Vibrational vector of the 346.7 cm^{-1} mode.

Soret excitation. However, (normally forbidden) oop modes also acquire rR enhancement when oop distortion is present in the porphyrin skeleton.[12] The oop pyrrole-tilting distortion occurs in the H-NOX heme model (Figure 1B), which can enhance resonance Raman activities of oop pyrrole-tilting modes specifically. There exist three such modes, i.e., γ_6 (A_{2u}), γ_{16} (B_{2u}), and γ_{23} (E_g).[13] Here, the symmetry representations for the idealized D_{4h} porphyrin are given in parentheses. The mode vectors of these are well described for the reference CO·Fe(OMP)·Im (Figure S1[18]). It should be noted that, due to the asymmetric axial ligation of Im and CO in this reference system, Fe is slightly displaced from the mean porphyrin plane toward CO by 0.04 Å (Figure S2[18]). As results, γ_6 is mixed with ν_8 (A_{1g} ip mode), whereas γ_{23} with ν_{50} and ν_{51} (E_u ip modes), as shown in Figure S1.[18] Hence, γ_6 and γ_{23} can be strongly enhanced with Soret excitation via the mixing with ip modes as well as the oop porphyrin distortion and are the most likely candidates for the 312 cm^{-1} Raman band.

In order to extract γ_6/ν_8, γ_{23}/ν_{50}, and γ_{23}/ν_{51} characters in the H-NOX heme modes, we calculated inner products of the porphyrin mode vectors between CO·Fe(OMP)·Im and the H-NOX heme after superposition of the two structures using the common porphyrin atoms and then picked up the modes that have both a high polarizability derivative value (>5 $Å^4\,amu^{-1}$) and a high correlation value (>0.1) with either of the γ_6/ν_8, γ_{23}/ν_{50}, or γ_{23}/ν_{51} of CO·Fe(OMP)·Im. Here, the inner product (correlation) values were normalized in a subspace composed of the 81 modes below 400 cm^{-1}.

As a result, we found four modes that satisfied the above conditions: 226.8 (0.119 with γ_6/ν_8, 8.3 $Å^4\,amu^{-1}$), 331.3 (0.102 with γ_{23}/ν_{50}, 12.4 $Å^4\,amu^{-1}$), 346.7 (0.294 with γ_{23}/ν_{50}, 7.4 $Å^4\,amu^{-1}$), and 383.3 cm^{-1} (0.138 with γ_{23}/ν_{50}, 8.8 $Å^4\,amu^{-1}$), which are marked with arrow heads in Figure 2A. Here, the calculated frequencies are italicized for clarity. The 331.3 and 383.3 cm^{-1} modes also have correlation with γ_6/ν_8 (0.086 and 0.098 correlation values, respectively). In the rR spectrum of 6c sGC–CO with YC-1, strong bands also occur at 346 and 371 cm^{-1}, which have been assigned to ν_8 and propionate bending, respectively.[5] The 331.3 cm^{-1} mode should correspond to the 346 cm^{-1} Raman band (ν_8) due to its γ_6/ν_8 character and near frequency coincidence, whereas the 383.3 cm^{-1} mode to the 371 cm^{-1} Raman band (propionate bending) (Figure S3[18]). Indeed, the 383.3 cm^{-1} mode contains oop 6-propionate bending as the primary component, accompanied by oop tilting of the pyrrole A.

It is worth mentioning that ν_8 and the propionate bending are well known because they normally give strong intensities in Soret-rR spectra of various heme proteins. We found that, when the heme iron is ligated by CO and His, ν_8 is mixed with γ_6, as exhibited in CO·Fe(OMP)·Im (Figure S1A[18]). In addition, the mode correlation analysis elucidates that this mode is further mixed with γ_{23}/ν_{50} when the pyrrole ring is tilt. This complexity has never been recognized because heme band assignments have been usually made based on the conventional mode classification using 4c nickel(II)–porphyrins,[14] where ip and oop modes are essentially isolated. The mode correlation analysis also elucidates that the propionate bending is mixed with γ_{23}/ν_{50} and γ_6/ν_8. Such mixing with porphyrin vibrations must be the origin of the rR enhancement of the propionate mode.

The rest mode located at 346.7 cm^{-1} is assignable to the 312 cm^{-1} Raman band, though the order of the three bands is different from the experiment. Vibrational vector of the 346.7 cm^{-1} mode is shown in Figure 2B. The motion of this mode is fairly delocalized over the heme and residues, involving pyrrole tilting and propionate bending as well as CO and Im tilting and Fe translation. Arg NH_2-rocking and twisting are also seen. The calculated frequency (346.7 cm^{-1}) of this mode is somewhat deviated from the experimental value (312 cm^{-1}),

presumably due to the limitation of our current model for protein environments. This mode may be more delocalized over the protein moiety, which causes a frequency downshift. The systematic computation error in (harmonic) frequency analysis is also a partial reason for the deviation, which is often corrected by a scaling factor.[15]

It should be noted that a possibility of the γ_7 (A_{2u}) assignment to the 312 cm^{-1} band, as noted previously,[16] is unlikely. γ_7 is methine wagging (Figure S1E[18]), usually enhanced in 5c domed heme spectra. Moreover, the H-NOX heme mode correlated with γ_7 (0.735 correlation) at 358.4 cm^{-1} does not have a high polarizability derivative value (2.5 $Å^4\,amu^{-1}$) or the mixing with any ip mode (Figure S3C[18]).

In summary, we have identified a delocalized mode, including oop (γ_{23}) and ip (ν_{50}) porphyrin motions, as the most likely candidate for the newly observed Raman band enhanced in active sGC–CO. This assignment suggests that binding of YC-1 induces a displacement of the YxSxR residues, pulling down the pyrrole ring out of the plane through the propionate, which results in the γ_{23}/ν_{50} mode enhancement in the rR spectrum. We propose that such a displacement of the conserved residues is involved in the signaling.

The displacement of the YxSxR motif alters not only the heme planarity but also the π-back donation from Fe to CO through the hydrogen bonds with propionates, which induces frequency shifts of the Fe–CO stretching ($\nu_{Fe–CO}$) and C–O stretching ($\nu_{C–O}$) modes. When propionates are more neutralized (stronger hydrogen-bonding occurs), $\nu_{Fe–CO}$ shifts down and $\nu_{C–O}$ shifts up.[11b] Previous Raman and FTIR studies revealed that YC-1 shifts $\nu_{Fe–CO}$ from 475 to 488 cm^{-1} and $\nu_{C–O}$ from 1987 to 1972 cm^{-1}.[5,17] These experimental data are consistent with our proposal that YC-1 displaces the YxSxR motif, which lengthens the hydrogen bonds between Arg and the propionate.

Finally, it would be interesting to note that the delocalized mode includes both Arg and Im motions. Although the proximal heme environment is not fully incorporated into the current model, a coupling motion between the YxSxR motif and the proximal His may be important in light of the Fe–His bond cleavage in the case of NO binding.

This work was supported by a Grant-in-Aid for Young Scientists (A) Nos. 22685003 (to Y.S.) and 23685040 (to M.K.) from JSPS.

References and Notes

1 K. R. Rodgers, *Curr. Opin. Chem. Biol.* **1999**, *3*, 158.
2 Y. Zhao, J. P. M. Schelvis, G. T. Babcock, M. A. Marletta, *Biochemistry* **1998**, *37*, 4502.
3 T. Tomita, T. Ogura, S. Tsuyama, Y. Imai, T. Kitagawa, *Biochemistry* **1997**, *36*, 10155; J. R. Stone, M. A. Marletta, *Biochemistry* **1996**, *35*, 1093.
4 A. Friebe, G. Schultz, D. Koesling, *EMBO J.* **1996**, *15*, 6863.
5 B. Pal, K. Tanaka, S. Takenaka, T. Kitagawa, *J. Raman Spectrosc.* **2010**, *41*, 1178.
6 M. Koglin, S. Behrends, *J. Biol. Chem.* **2003**, *278*, 12590.
7 P. Pellicena, D. S. Karow, E. M. Boon, M. A. Marletta, J. Kuriyan, *Proc. Natl. Acad. Sci. U.S.A.* **2004**, *101*, 12854.
8 D. S. Karow, D. Pan, R. Tran, P. Pellicena, A. Presley, R. A. Mathies, M. A. Marletta, *Biochemistry* **2004**, *43*, 10203.
9 M. J. Frisch, G. W. Trucks, H. B. Schlegel, G. E. Scuseria, M. A. Robb, J. R. Cheeseman, G. Scalmani, V. Barone, B. Mennucci, G. A. Petersson, H. Nakatsuji, M. Caricato, X. Li, H. P. Hratchian, A. F. Izmaylov, J. Bloino, G. Zheng, J. L. Sonnenberg, M. Hada, M. Ehara, K. Toyota, R. Fukuda, J. Hasegawa, M. Ishida, T. Nakajima, Y. Honda, O. Kitao, H. Nakai, T. Vreven, J. A. Montgomery, Jr., J. E. Peralta, F. Ogliaro, M. Bearpark, J. J. Heyd, E. Brothers, K. N. Kudin, V. N. Staroverov, R. Kobayashi, J. Normand, K. Raghavachari, A. Rendell, J. C. Burant, S. S. Iyengar, J. Tomasi, M. Cossi, N. Rega, J. M. Millam, M. Klene, J. E. Knox, J. B. Cross, V. Bakken, C. Adamo, J. Jaramillo, R. Gomperts, R. E. Stratmann, O. Yazyev, A. J. Austin, R. Cammi, C. Pomelli, J. W. Ochterski, R. L. Martin, K. Morokuma, V. G. Zakrzewski, G. A. Voth, P. Salvador, J. J. Dannenberg, S. Dapprich, A. D. Daniels, Ö. Farkas, J. B. Foresman, J. V. Ortiz, J. Cioslowski, D. J. Fox, *Gaussian 09 (Revision A.02)*, Gaussian, Inc., Wallingford, CT, **2009**.
10 A. Schäfer, H. Horn, R. Ahlrichs, *J. Chem. Phys.* **1992**, *97*, 2571.
11 a) M. Ibrahim, C. Xu, T. G. Spiro, *J. Am. Chem. Soc.* **2006**, *128*, 16834. b) C. Xu, M. Ibrahim, T. G. Spiro, *Biochemistry* **2008**, *47*, 2379.
12 M. Kubo, F. Gruia, A. Benabbas, A. Barabanschikov, W. R. Montfort, E. M. Maes, P. M. Champion, *J. Am. Chem. Soc.* **2008**, *130*, 9800; A. A. Jarzęcki, T. G. Spiro, *J. Phys. Chem. A* **2005**, *109*, 421; D. Li, D. J. Stuehr, S.-R. Yeh, D. L. Rousseau, *J. Biol. Chem.* **2004**, *279*, 26489.
13 S. Hu, K. M. Smith, T. G. Spiro, *J. Am. Chem. Soc.* **1996**, *118*, 12638.
14 M. Abe, T. Kitagawa, Y. Kyogoku, *J. Chem. Phys.* **1978**, *69*, 4526; T. G. Spiro, P. M. Kozlowski, M. Z. Zgierski, *J. Raman Spectrosc.* **1998**, *29*, 869.
15 M. W. Wong, *Chem. Phys. Lett.* **1996**, *256*, 391.
16 E. Martin, K. Czarnecki, V. Jayaraman, F. Murad, J. Kincaid, *J. Am. Chem. Soc.* **2005**, *127*, 4625.
17 R. Makino, E. Obayashi, N. Homma, Y. Shiro, H. Hori, *J. Biol. Chem.* **2003**, *278*, 11130.
18 Supporting Information is available electronically on the CSJ-Journal Web site, http://www.csj.jp/journals/chem-lett/index.html.

